



Thermoelectric Characteristics of Bi₂S₃-Based Sandwich Materials

Riyadi Muslim¹, Ganjar Pramudi¹, Dimas Adika¹, Catur Harsito^{1,2*}

¹ Mechanical Engineering of Vocational School, Sebelas Maret University, Surakarta 57126, Indonesia

² Department of Mechanical Computer Industrial and Management Engineering, Kangwon National University, Samcheok-si 24341, Republic of Korea

Corresponding Author Email: catur_harsito@staff.uns.ac.id

Copyright: ©2025 The authors. This article is published by IIETA and is licensed under the CC BY 4.0 license (<http://creativecommons.org/licenses/by/4.0/>).

<https://doi.org/10.18280/ijepm.100111>

ABSTRACT

Received: 7 June 2024

Revised: 28 October 2024

Accepted: 21 March 2025

Available online: 31 March 2025

Keywords:

sandwich material, thermoelectric, single module, electric characteristics

Thermoelectric are a very interesting source of electrical energy. There is a lot of exploration about the use of thermoelectric and the potential that exists. Thermoelectric materials are of particular concern to obtain better efficiency. This research aims to investigate the performance of a novel thermoelectric generator (TEG) design based on Bi₂S₃ sandwich materials through numerical investigation. Key focus areas include power output, efficiency, compatibility for future applications, and temperature distribution characteristics. Data shows that this design has increased efficiency by 4.2%. When performing experimental setup, it is important to offer more reliable data quality, these simulation results offer a pre-plenum data approach to minimize omissions.

1. INTRODUCTION

The energy transformation phenomenon has brought about new challenge and opportunity, exclusively for thermoelectric field [1]. Thermoelectric is kind of energy generator that convert thermal into electricity. It offered direct conversion of temperature difference into electric potential between each material pair junction, called Seebeck Effect [2]. This invention has widely use both industrial and non-industry known as Thermoelectric Generator (TEG) [3], which mentioned more compact, free-noise, and quite suite for hybrid mode electric generator [4]. The application is to utilize waste engine heat in combustion engines [5] and exhaust gas heat [6] as an electricity generator. Many researchers concerned this technology more environmentally refer to global warming problem [7]. Thermoelectric technology is one of the green energy source converters that can provide electrical energy to electric and electronic systems [8]. Even thermoelectric was possible generated form human body [9]. According to this issue, thermoelectric are amongst the most promising solid state energy generator by using low temperature for further investigated.

While fuel energy has important role, thermoelectric has been known as thermal production into electricity which offer efficiency in some selective applications purpose. It demands expanding thanks to their long-life operation under extreme conditions without requiring maintenance [10, 11]. Constructing a theory-generating device (TEG) with theoretical efficiency is a huge step forward in the research, especially given the multiple concrete hurdles [8]. Furthermore, this device suite to various waste heat recovery

systems [12, 13]. As a result, the advancement of TE materials necessitates ongoing work from material scientists, physicists, chemists, and theory scientists [14].

The growing demand for devices capable of more efficient electrical energy conversion has intensified researchers' interest in thermoelectric technology. The potential for positive growth in Thermoelectric Generators (TEGs) presents both opportunities and challenges for innovative development [10]. Currently, there are six key areas that can be further developed: materials, design, reliability, durability, figure of merit, and temperature difference (ΔT) [12]. These areas can be combined with various configurations such as quantity, structure, combination, series connection, shape, range, pick-up points, environmental conditions, and installation types on specific objects. This field of research still offers numerous opportunities for exploration.

This material sandwich structure is one of the most established TEG fabrication structures worldwide, enhancing the thermoelectric properties by way of enhancing heat distribution and efficiency in energy conversion. The structure allows for more intensive thermal concentration that may be distributed at the heat source; hence, it provides maximum voltage generation with better efficiency [15]. The good quality of the thermal interface in the sandwich structures ensures that on the hot side, effectively there is a heat concentration, which directly contributes to enhancing the conversion of heat to electricity [16]. By selecting appropriate materials for sandwiches with high thermal conductivity and good thermoelectric properties, one achieves high power density and hence a good flow of electrons, ensuring higher thermoelectric performances [17]. As expected, this setup

increased electron transport according to Zhang et al. [18], this is the most important factor for increasing the output power of thermoelectric generators.

Recent study about thermoelectric with related material structure, thermoelectric model with different sandwich material module characteristics has been developed in this research. To find out what output phenomena are produced, 3D modeling and simulation using an application will be discussed. The purpose of this research is to reveal:

- Power output phenomenon of this designed model
- Efficiency offers of this novelty
- Compatibly of this designed model as a TEG for further generation
- Temperature distribution characteristic

The parameters specification and the prediction results of the issued calculations are further explained in this paper.

2. METHODOLOGY

There are three related theories of thermoelectric operation that are popular among researchers. These are the Seebeck Effect, the Peltier Effect, and the Thomson Effect. TEG operation occurs when two poles experience a temperature difference that leads to the production of kinetic energy. TEG operation means that when one side of a metal is heated while the other side is cooled, the electrons surrounding the metal atoms on the hot side of the metal have more energy than the corresponding electrons on the cooler side. Thus, it is possible that the hot electrons will have more kinetic energy than the cooler electrons. Generally, these poles consist of two pairs of metal plates called P-type and N-type semiconductors. In principle, the use of this technique is not able to create a large voltage (V), even though various concepts of series or parallel circuits have been carried out which combine the two. This is affected by the connector or connecting material used to combine metal plates (poles) which are also made of metal. This situation influences the direction of stress created by the main material.

Firstly, introduced by Thomas Johan Seebeck in the 1820s, the system is defined as a mechanical system in which a temperature difference produces a voltage, known as the Seebeck effect [14]. A voltage gap (gap potential) can occur in the fusion of semiconductor poles which carry opposite temperature gradients (ΔT). Temperature changes occur on both sides of the semiconductor plate where the substance is cooled or heated. This cold to hot change or vice versa, generates kinetic energy which creates an electrical voltage that can be utilized. The theory can be formulated as:

$$S = -\frac{\Delta V}{\Delta T} \quad (1)$$

The Seebeck effect (S) is the very basis of TEGs, wherein a temperature difference across a material induces an electric potential. For thermoelectric materials, the Seebeck coefficient measures voltage per unit temperature difference. A higher Seebeck coefficient improves voltage output for a given temperature gradient [19, 20]. Bi_2Te_3 -based thermoelectric materials hold promise for their potential energy harvesting in thermal-to-electrical energy conversion and also for cooling. Doping with elements such as Sn in Bi_2Se_3 nanosheets has improved Seebeck coefficients and reduced thermal conductivity [21]. Other approaches include

the introduction of dense dislocation arrays, dispersion of nano-SiC particles [22], and topological insulator boundary states studies in Bi_2Te_3 thin films for potential thermoelectric improvements [23]. These developments will lead to even higher values of ZT and optimized temperature ranges for both N-type and P-type materials in thermoelectric devices.

Thermoelectric simulations should consider the dimensions of the TEG as a problem-solving analysis and usually consist of elements P-legs and N-legs. When the process enters steady state, all the energy is transferred through the hot side pole and released at the cold side junction. It is characterized by constant temperature gradients and steady heat flows from hotter to colder poles. To define the power flowing through both sides (hot side and cold side) of the module, we can calculate according to study [24]:

$$P_c = n \left[IT_h a - \frac{1}{2} I^2 R + K(T_h - T_c) \right] \quad (2)$$

$$P_h = n \left[IT_h a - \frac{1}{2} I^2 R + K(T_h - T_c) \right] \quad (3)$$

To be able to calculate the power generated on both sides, we need to calculate the Seebeck coefficient (a). Meanwhile, in the derivation stage, it is possible to ignore heat loss and heat and electricity contact resistance. This step is enough to calculate the power passing through each module. The formulas for the a , thermoelectric resistance (R), and thermal conductivity (K) can be expressed as [25, 26]:

$$a = (a_p - a_n) \quad (4)$$

$$R = \frac{\rho_{pL}}{A_p} - \frac{\rho_{nL}}{A_n} \quad (5)$$

$$K = \frac{1}{L} (K_p A_p + K_n A_n) \quad (6)$$

Considering the external load resistance (R_L) and the current (I) generated in the system, the generated output power can be calculated as:

$$P_h - P_c = W = I^2 R_2 \quad (7)$$

$$I = \frac{a(T_h - T_c)}{R + R_L} \quad (8)$$

TEG Module can be analyzing the efficiency offer as,

$$\eta = \frac{(P_h - P_c)}{P_h} = \eta_c \frac{\beta}{(1 - \beta) + (1 + \beta)^2 (ZT_h)^{-1} \eta_{c/2}} \quad (9)$$

Refer to single thermoelectric characteristic by using single leg with TE material, where $\beta = \frac{R_L}{R}$, $Z = \frac{a^2}{RK} = \frac{a^2}{PK}$, and considering efficiency formula $\eta = \frac{T_h - T_c}{T_h}$, it can be calculate that optimum efficiency at $\beta = \frac{R_L}{R} = \sqrt{1 + Z\bar{T}}$ as follow:

$$\eta_{max} = \frac{T_h - T_c}{T_h} \left[\frac{\sqrt{1 + Z\bar{T}} - 1}{\sqrt{1 + Z\bar{T}} - \frac{T_c}{T_h}} \right] \quad (10)$$

\bar{T} in this calculation means the average between T_h and T_c .

The Thomson effect became the next development theory, introduced for the first time by an English physicist named William Thomson (1854). The core of this concept lies in the use of a single plate of material that has a temperature difference along its current circuit. This concept allows you to measure the current flowing through the plate and the amount of heat loss caused by the temperature difference. This distinguishes it from his previous two concepts.

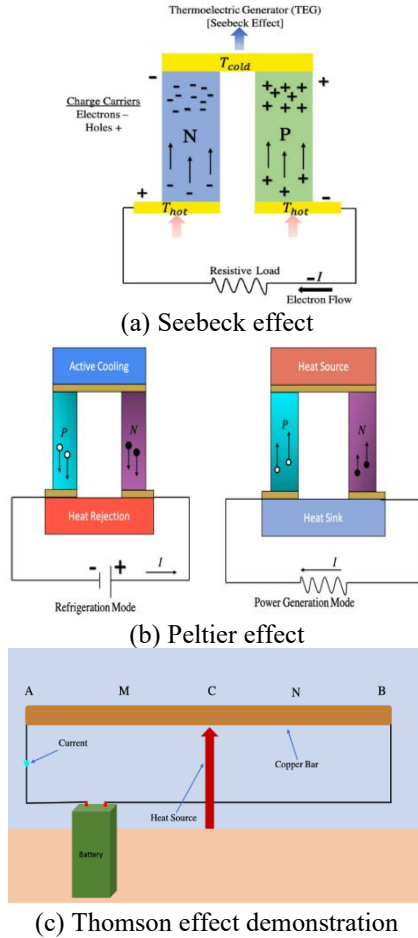


Figure 1. Thermoelectric working principle [14]

Numerical modeling and simulations are used in this study as detailed prediction methods for TE performance. The design framework for the proposed idea plan was created using the Solidwork software application, and the numerical analysis was performed using the ANSYS software application. This application is widely used by researchers for modeling studies in various fields such as materials, CFD, stress, torsion, FEM and others [27-30]. References for setting the input parameters for this modeling are given in Table 1. These parameters serve as a reference for possible variations to find the best performance. To explain the thermoelectric concept, a geometric adjustment is required as seen in Figure 1. The development of this model is the result of an analysis of previous studies using different material types, different temperature regimes, stacked with the material sandwich concept. Materials ($\text{Cu}_2\text{Se}+$; $\text{BiTe}+$) (Bi_2S_3- ; $\text{CuFeS}-$) were used for leg 1 and ($\text{PbSe}+$; $\text{BiTe}+$) (Bi_2S_3- ; $\text{AgInSe}-$) were used for leg 2 with a temperature range (ΔT) of 300–1000K. The module height plays an important role in supplying the moving energy in the thermoelectric circuit, being the part to be analyzed.

Table 1. Simulation variation set-up

Series	Module Height (mm)	Range Hot Side
(A1)	10	300-1000
($\text{Cu}_2\text{Se}+$; $\text{BiTe}+$)	15	
(Bi_2S_3- ; $\text{CuFeS}-$)	20	
(A2)	10	
($\text{PbSe}+$; $\text{BiTe}+$)	15	
(Bi_2S_3- ; $\text{AgInSe}-$)	20	

In this study, a new thermoelectric module structure is designed. Dimension plays important role to the result performance. It predicts absorb area to produce energy, further it should suite with the installation device. Through electrodes, the P and N type legs were thermally coupled in series (as opposed to electrically in parallel), as shown in Figure 2. The geometries under investigation consisted rectangular shape as standard leg geometry chosen. Furthermore, Table 2 shows the module dimension requirement of this numerical study. Simplified calculation and evaluation of the generator's thermoelectric properties. It was discovered that thermoelectric materials have thermal conductivity, and it was investigated how temperature fields cause the diffusion of thermoelectric material carriers from high temperature to low temperature.

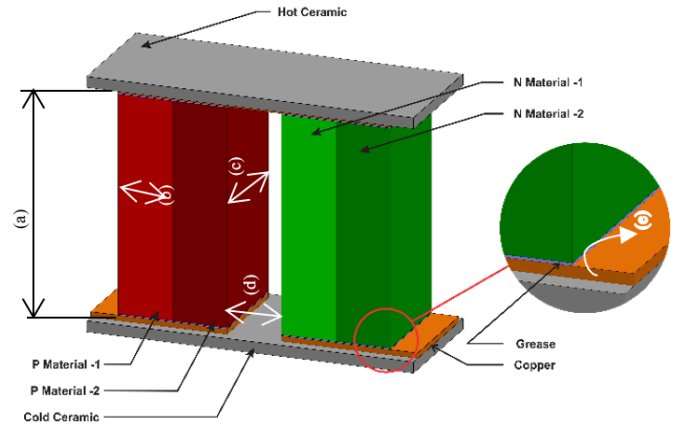


Figure 2. Schematic thermoelectric module

Table 2. Module dimension

Module Dimension	Value (mm)	Symbol
(a) TE leg height		H
(b) TE leg width	1.4	W
(c) TE leg length	1.4	L
(d) Spacing between legs	1.0	D
(e) Substrate thickness	0.8	

This numerical simulation modeling goes through several stages, one of which is meshing. This meshing stage is carried out with a hexagonal mesh shape. The size element is set to capture the phenomena that occur. In the copper and ceramic parts, the mesh size is made at a thickness of 0.01 mm and 0.05 mm respectively, while in the leg part it is made with a size of 0.1 mm with a global mesh size of 0.1 mm [31].

3. EXPERIMENTAL SETUP

3.1 Validation

A validation conducted in this work to eliminate

uncertainties regarding the accuracy of the results obtained. The above equations combined with the sandwich material method can be used to simulate the heat transfer performance of thermoelectric elements (refer to Table 3). This study has similar requirements for prior research references as validation. The data is within the 5% maximum source accuracy level according to process validation, while it consists of an error value at 1.5%. Therefore, the model used in this study is believed to be accurate and reliable for determining mathematical modeling of thermoelectric performance [32].

3.2 Material properties

Material selection is the first step in modeling. The material properties are the basic set-up parameters, so that calculations can be directly calculated. This modeling uses selected materials in the following format: (a) BiTe+, (b) Cu₂Se+, (c) PbSe+, (d) Bi₂S₃-, (e) CuFeS-, and (f) AgInSe. Material preferences used consider three things, namely: thermal conductivity, electrical resistivity, and owned thermo-power. Figure 3 provides an illustration of the material criteria used in this simulation. Preliminary studies conducted show that the

selected materials currently offer the best performance and are suitable for use as either P-type or N-type. In this work, a semiconductor plate is placed in series between two metal plates, hot and cold.

Each material has its own unique characteristics. Some specs have the same trendline and may reach different peak values. In contrast, some show different trend lines on both the hot and cold sides. We can observe in Figure 3 material properties (a) BiTe+, (b) Cu₂Se+, (d) Bi₂S₃-, (e) CuFeS-, have a thermopower trend-line that tends to increase with increasing temperature. On the one hand, there is a downward trend-line in the thermal conductivity values of the material (c) PbSe+, (d) Bi₂S₃-, (e) CuFeS-, (f) AgInSe. On the other hand, we can explain that the electric resistance of the six materials varies greatly. Some specs support it, others contradict it. In this case we can configure the material based on the specific performance that we want to optimize. For example, the combination of (b) Cu₂Se+ and (f) AgInSe materials can generate large thermoelectric voltages as the temperature trend line increases compared to other types of materials based on their properties. Based on this material property data, the basis for the configuration design of modules A1 and A2 is formed according to Table 1.

Table 3. Validation

Variable	Erturun and Mossi [33]	Harsito et al. [34]	This Research
Voltage (V)	8.70E-02	8.70E-02	8.70E-02
Current Generated (mA)	328.00	326.00	326.85
Power Generated (mW)	28.50	28.00	28.44
Heat Absorbed (mW)	673.00	671.59	672.95
Efficiency (η)	4.235%	4.169%	4.226%

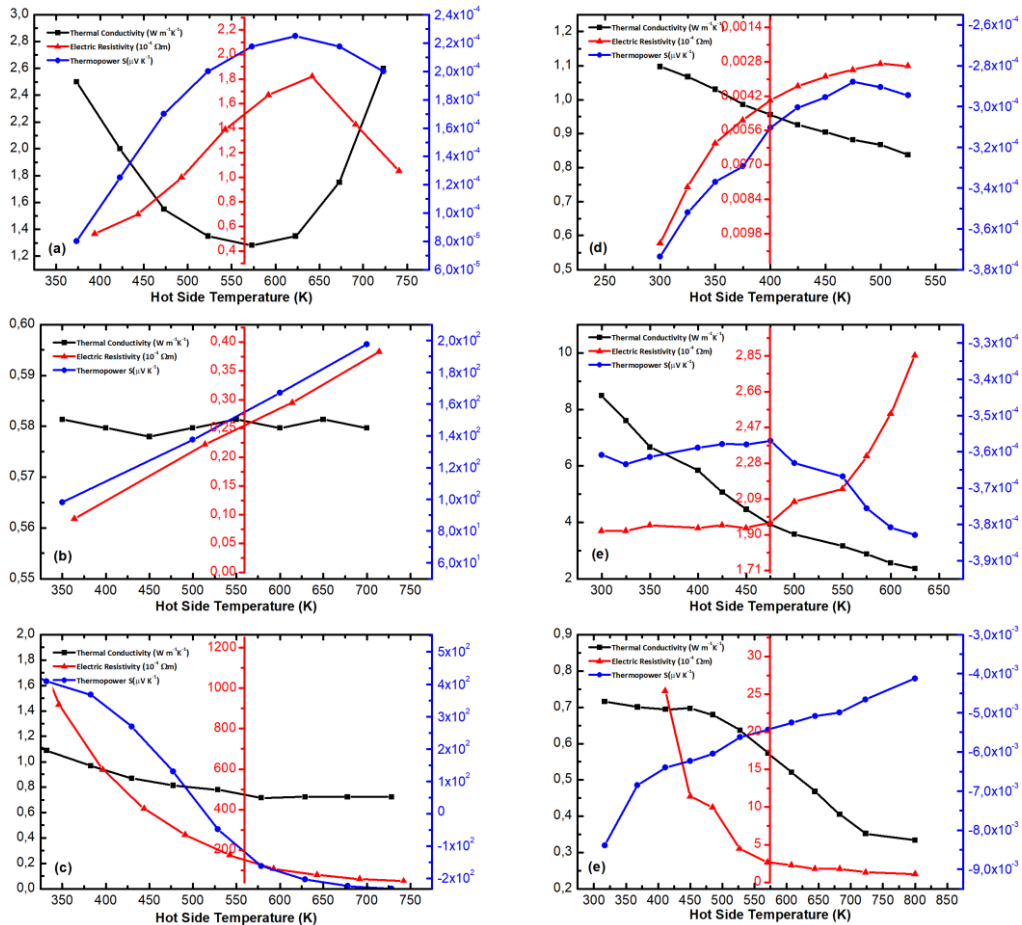


Figure 3. Material properties (A) BiTe+, (B) Cu₂Se+, (C) PbSe+, (D) Bi₂S₃-, (E) CuFeS-, (F) AgInSe

In Figure 3, the Y-axis includes three distinct parameters, each represented with a different color and scale. It is thermal conductivity (black line) with unit $W m^{-1}K^{-1}$, electrical resistivity (red line) with unit $10^{-4} \Omega m$, and thermopower or seebeck coefficient (blue line) with unit $\mu V K^{-1}$.

In order to verify the feasibility of the Thermoelectric by using sandwich material which has material properties BiTe+, Cu₂Se+, PbSe+, Bi₂S₃-, CuFeS-, and AgInSe- were measured as a function of the temperature difference and the curves are shown in Figure 3. The source for the differences in thermal conductivity arises from several factors. Clearly, every thermoelectric material conducts different changes in thermal conductivity with regard to temperature variations. Indeed, Bi₂S₃ and BiTe⁺-based materials are more likely to demonstrate nonlinear responses to temperature variation as a result of variation in phonon scattering, lattice vibration, and electron-phonon interaction. This effect can take place in materials such as Bi₂S₃ under the first working condition, leading to significant deviation from other conditions. The quality of the thermal interface greatly affects heat transfer in sandwich-structured TEGs. Under a high-temperature gradient or some other certain conditions, the thermal interface resistance between layers takes great effect. So, the most reasonable reason affecting temperature differences is the thermal properties and interface quality. Each material has thermal conductivity characteristic which offer electrical

resistivity and thermo-power performance that needed for further analyze.

4. RESULT DISCUSSIONS

4.1 Power output

Analysis of power generation was done by mathematical calculations. Modeling was carried out step by step considering the running process according to the specifications. Temperature raw material data was categorized according to data collection criteria under the same constraints. In order to get perfect comparison results, a simulation was repeated to see the visibility of the data while still considering the material specifications and the designed geometric model. Data analysis is performed critically and carefully to minimize various aspects of possible errors. The output power produced by the module is shown in Figure 4. It can be clearly seen that the difference in the sandwich material of the thermoelectric legs affects the output. Configuration A1 gives better results than configuration A2. However, they both show the same trend line trend pattern. The height of the modules that produce the best performance in configurations A1 and A2 equals $t=10$ mm. However, module A shows a more optimal performance effect.

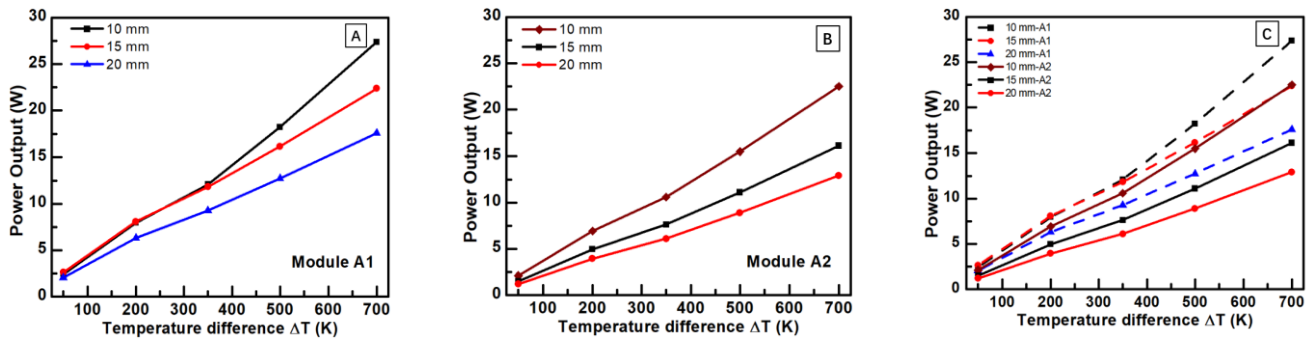


Figure 4. Power output (A) Module A1, (B) Module A2, (C) Module A1 vs Module A2

Output power is the basis of the first consideration when choosing a TEG [35]. In principle, the temperature distribution (ΔT) can also be widened by excessive leakage. This condition can have a direct impact on material conditions such as: warping, stress, and even damage to other components. Every material can experience degradation of properties as a result of the shock of flowing heat [36]. The worst risk is causing the device to not function. Sufficiency of power is another factor so that it can be installed on certain objects. Optimal selection of modules with good thermal conductivity minimizes the occurrence of Joule heating (temperature rise due to current flowing through the circuit). The performance trend results show that the material is of safe specification. This result is suitable for use as a low to medium power generator.

Figure 5 shows the relationship between current and generated power. This module provides an interesting and diverse set of criteria. We can use the A1-10 mm configuration for low current TEG with large power. Simultaneously we can use A2-10 mm and A1-15 to achieve large currents with optimum power. A2 is the lowest specification of the configuration displayed. The displayed power output gives a positive outlook and has a significant impact according to the

thermoelectric instrument in operation. The optimum power that can be generated is 27.385 Watt, while the optimum current that can be achieved is 700 mA. One of the CuFeS-containing A1 building materials has a relatively low thermoelectric power as shown in Figure 6, but the sandwich diffusion process with other materials does not affect the performance degradation. A2 contains a PbSe+ constituent material, while A2-20 has low performance. The most optimum module height to produce maximum power is at 10 mm, both A1 and A2. The presence of the AgInSe- component in A2 shows that a low electric resistivity value can decrease the performance of the power generated.

The thermal conductivity value also affects the voltage generated. Higher thermal conductivity has a greater impact on the voltage that can be generated. The A1-10 configuration provides maximum performance, this is in line with the supporting material properties that have good thermal conductivity. In contrast, the A2-20 module has the lowest output, but is still within the ideal voltage range. This graphic makes it clear that the designed module is suitable for further development.

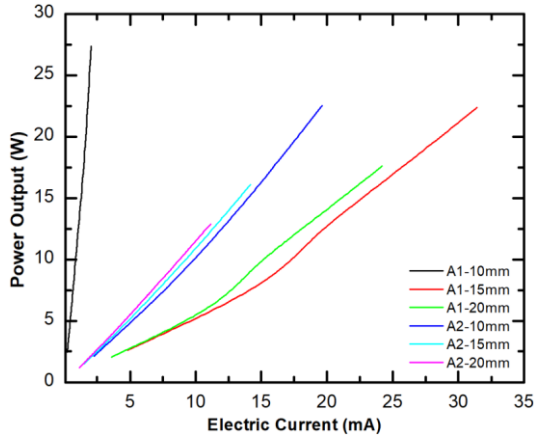


Figure 5. Power output vs. Ampere

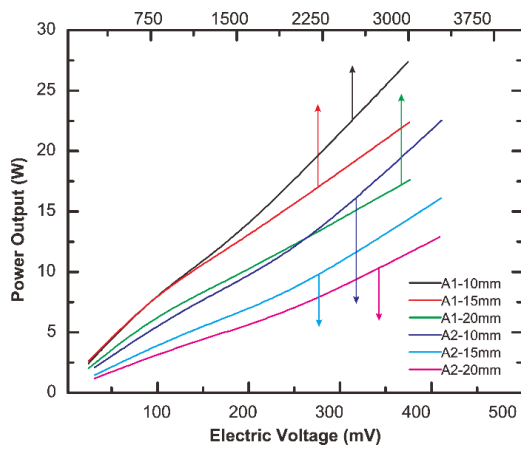


Figure 6. Power output vs. electric voltage

4.2 Efficiency

Figure 7 shows the designed model efficiency data. Material composition can significantly improve efficiency. The geometric design is suitable for conducting electricity with temperature differences between 300° and 1000°K. The chart confirms that the designed module configuration has a positive impact on increasing power output and is suitable for manufacturing. Although TEG efficiency is generally lower than other energy sources, its use remains popular. The main reason for the numerous studies related to this is that the tool can withstand extreme conditions without any special precautions [8]. Choosing a material with good thermal conductivity helps increase TEG efficiency. Furthermore, the choice of N-type or P-type material affects the ability to absorb temperature, improving efficiency [24].

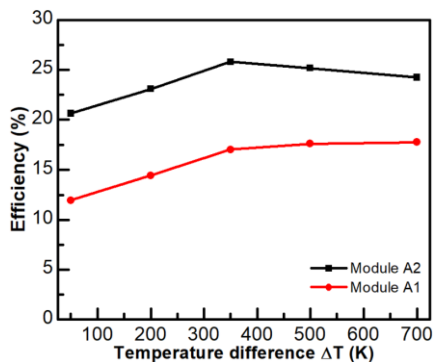


Figure 7. Efficiency

4.3 Compatibility

Compatibility analysis is used to check the eligibility of modules for using as TEG configurations. Figure 8 shows the estimated material compatibility of N-type and P-type. Both have different compatibility factors, but the difference is greater than 2, indicating a normal criterion. The s-factor and z addition play an important role in the efficient operation of TEGs and are very reasonable criteria for choosing TE materials designed for a particular engineered device. At the N pole, Bi_2S_3 is known to fail to reach the optimum temperature, but the trend is decreasing. On the other hand, CuFeS_2 in the graph actually gives a positive interaction. The condition of the chart shows the variations in the trend of the changing data for both N-type and P-type. Simulation data show that the TE material can be used as a leg-TEG configuration.

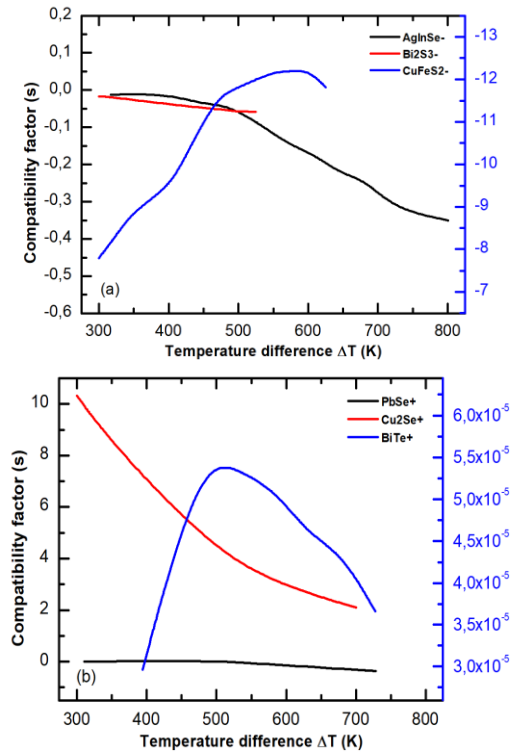


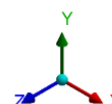
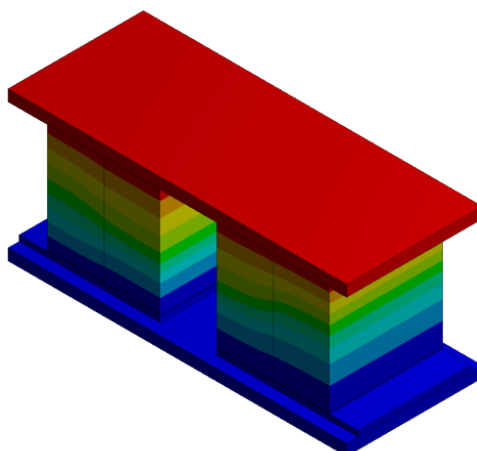
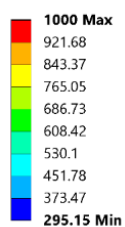
Figure 8. Compatibility factor of material (a) N-type, (b) P-type

4.4 Temperature distribution

The module flow temperature indicates a thermal degradation of heat per unit volume. The resulting internal heat plays an important role in determining the amount of contact resistance in the binderies during the process. Figure 9 shows that the distribution is influenced by the constituent materials used. Module thickness affects the color degradation that occurs. With increasing material thickness, the temperature on the cold side of the TEG will be reduced due to increasing thermal resistance of the thickness. In effect, this spreads the temperature gradient across the thickness to make it much more gradual, hence making the distribution of heat somewhat much more uniform and avoiding hotspots. This is not meant to imply 'normal', but rather a more smooth and controlled temperature gradient. Those data performed, was analyzed by using ANSYS's software, where it's the temperature distribution was generated using finite element analysis, commonly used to simulate thermoelectric heat transfer and thermal effects.

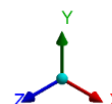
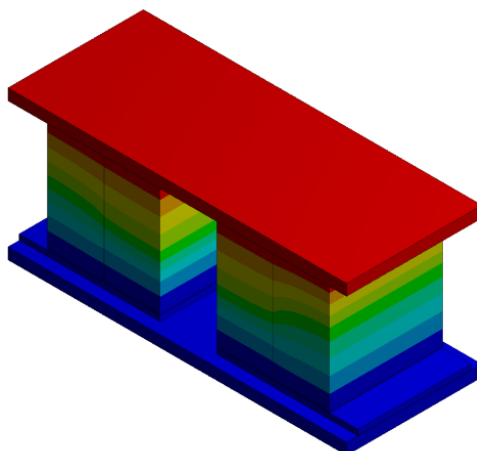
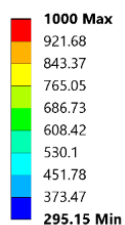
F: 10. (CuSe+;BiTe+) (Bi2S3-;CuFeS-)

Temperature
Type: Temperature
Unit: K
Time: 14
4/6/2023 9:50 PM



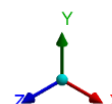
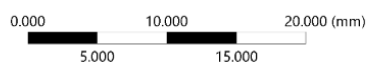
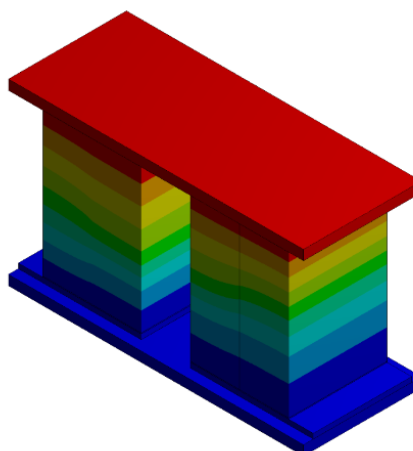
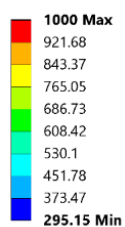
G: 10. (PbSe+;BiTe+) (BiS-;AgInSe-)

Temperature
Type: Temperature
Unit: K
Time: 14
4/6/2023 9:51 PM



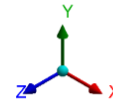
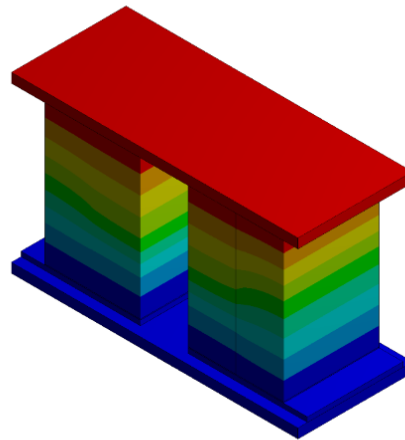
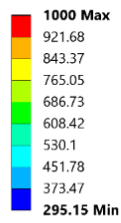
J: 15. (CuSe+;BiTe+) (Bi2S3-;CuFeS-)

Temperature
Type: Temperature
Unit: K
Time: 14
4/6/2023 9:56 PM



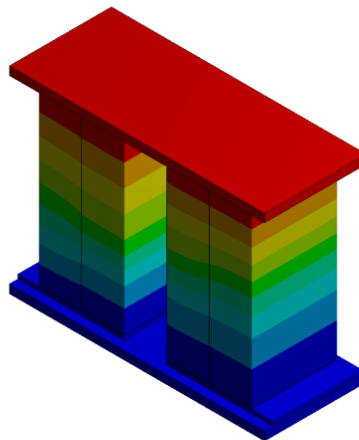
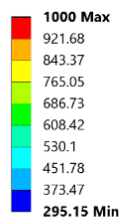
H: 15. (PbSe+;BiTe+) (BiS-;AgInSe-)

Temperature
Type: Temperature
Unit: K
Time: 14
4/6/2023 9:53 PM



K: 20. (CuSe+;BiTe+) (Bi2S3-;CuFeS-)

Temperature
Type: Temperature
Unit: K
Time: 14
4/6/2023 9:58 PM



I: 20. (PbSe+;BiTe+) (BiS-;AgInSe-)

Temperature
Type: Temperature
Unit: K
Time: 14
4/6/2023 9:54 PM

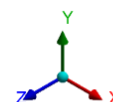
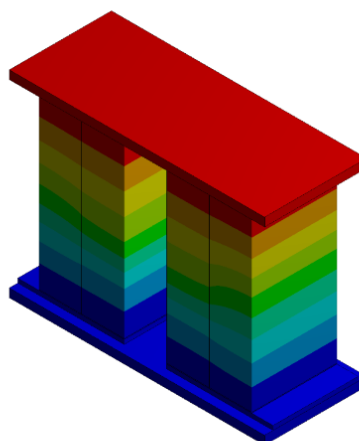
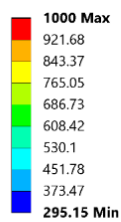


Figure 9. Temperature distribution

The combination of F10, there appears to be a proper distribution of temperature gradient with respect to the module. This even distribution could arise due to the inherent good thermal conductivity in the layers Cu_2Se and BiTe , allowing heat to pass through with relatively less hindrance. On the cold side, the presence of Bi_2S_3 and Cu_2FeS introduces some resistances that could balance the thermoelectric efficiency to hold more heat on the hot side and maintain the gradient.

According to G10, the temperature distribution remains very close to the previous one, but with a little twist: substitution including PbSe and AgInSe could contribute to an increase in thermal resistance at some interfaces, which, in turn, might improve the thermoelectric effect due to a reduction in heat leakage. Consequently, there is an increased temperature gradient in certain regions of the thermoelement, which would be helpful for power generation since this increases the effective temperature difference across the thermoelectric elements.

In the case of J15, the thermal distribution in this configuration is uniform, similar to F10. It may indicate that the thermal properties are consistent within the layers of Cu_2Se and BiTe . This can be an indication that the involved combination serves well for heat transfer without losing much thermoelectric gradient. Further, H15 is also similar to G10 in giving a temperature distribution that is more variant, with a great drop of temperature across the thermoelectric layers. Perhaps this could be due to increased thermal resistance caused by the presence of AgInSe and its different thermal properties, which is good for maintaining a strong temperature gradient.

It can be observed from these simulations that all the different configurations give different effects to the temperature distribution and further affect the thermoelectric efficiency. The configurations with AgInSe and Bi_2S_3 have higher gradients, which means higher thermal resistance and thus should help in the thermoelectric effect. In turn, combinations such as $\text{Cu}_2\text{Se}+\text{BiTe}$ have less disparate heat flow that could be appropriate for applications needing balanced thermal dissipation. Further, this analysis supports the potential of Bi_2S_3 -based sandwich materials in enhancing TEG performance by carefully selecting material pairing to maximize temperature gradient retention along with energy conversion efficiency.

According to the explained data, the design of the TEG structure uses sandwich model combined with Bi_2S_3 material. This model has several advantages, including: minimalist structure, simplified shape, and an energy efficiency rate which tends to be 4.2% higher compared to previous research [14]. Furthermore, this design characteristic has possible production requirement, which mean relevant to industry demand for fabrication in large scale.

5. CONCLUSIONS

Comprehensive modelling of two module types with sandwich material geometries on a single thermoelectric has been carried out. Module A1 performs better than module A2 when combined material specifications for BiTe^+ , Cu_2Se^+ , PbSe^+ , Bi_2S_3^- , CuFeS^- , and AgInSe^- configurations. From the specifications of the material properties in the form of thermal conductivity, electrical resistivity, and thermo power produced, its result feasible to be an alternative material to

replace the standard thermoelectric leg either P-type or N-type. Leg variables with material configuration (Cu_2Se^+ ; BiTe^+) (Bi_2S_3^- ; CuFeS^-) have a good influence on the temperature distribution on the thermal plate as well as the thermoelectric characteristics that appear. The efficiency achieved by this module reaches 4.2%, which is better than previous studies. This configuration is suitable for manufacturing and provides

ACKNOWLEDGMENT

This work was supported by the Lembaga Penelitian dan Pengabdian kepada Masyarakat (LPPM) Universitas Sebelas Maret (UNS) (Grant No.: 194.2/UN27.22/PT.01.03/2024).

REFERENCES

- [1] Lu, X., Sun, P., Fan, D. (2023). Application of sliding mode predictive control in solar thermal power generation collector subsystem. *Journal of Applied Science and Engineering*, 26(10): 1481-1489. [https://doi.org/10.6180/jase.202310_26\(10\).0013](https://doi.org/10.6180/jase.202310_26(10).0013)
- [2] Huesgen, T., Woias, P., Kockmann, N. (2008). Design and fabrication of MEMS thermoelectric generators with high temperature efficiency. *Sensors and Actuators A: Physical*, 145: 423-429. <https://doi.org/10.1016/j.sna.2007.11.032>
- [3] Doraghi, Q., Khordehghah, N., Żabnieńska-Góra, A., Ahmad, L., Norman, L., Ahmad, D., Jouhara, H. (2021). Investigation and computational modelling of variable teg leg geometries. *ChemEngineering*, 5(3): 45. <https://doi.org/10.3390/chemengineering5030045>
- [4] Talawo, R.C., Fotso, B.E.M., Fogue, M. (2021). An experimental study of a solar thermoelectric generator with vortex tube for hybrid vehicle. *International Journal of Thermofluids*, 10: 100079. <https://doi.org/10.1016/j.ijft.2021.100079>
- [5] Ragupathi, P., Barik, D. (2023). Investigation on the heat-to-power generation efficiency of thermoelectric generators (TEGs) by harvesting waste heat from a combustion engine for energy storage. *International Journal of Energy Research*, 2023(1): 3693308. <https://doi.org/10.1155/2023/3693308>
- [6] Ragupathi, P., Barik, D., Vignesh, G., Aravind, S. (2020). Electricity generation from exhaust waste heat of internal combustion engine using Al_2O_3 thermoelectric generators. *Journal of Applied Science and Engineering*, 23(1): 55-60. [https://doi.org/10.6180/jase.202003_23\(1\).0007](https://doi.org/10.6180/jase.202003_23(1).0007)
- [7] Finn, P.A., Asker, C., Wan, K., Bilotti, E., Fenwick, O., Nielsen, C.B. (2021). Thermoelectric materials: Current status and future challenges. *Frontiers in Electronic Materials*, 1: 677845. <https://doi.org/10.3389/femat.2021.677845>
- [8] Bhuiyan, M.R.A., Mamur, H., Üstüner, M. A., Dilmaç, Ö.F. (2022). Current and future trend opportunities of thermoelectric generator applications in waste heat recovery. *Gazi University Journal of Science*, 35(3): 896-915. <https://doi.org/10.35378/gujs.934901>
- [9] Leonov, V., Torfs, T., Fiorini, P., Van Hoof, C. (2007). Thermoelectric converters of human warmth for self-powered wireless sensor nodes. *IEEE Sensors Journal*, 7(5): 650-657.

- <https://doi.org/10.1109/JSEN.2007.894917>
- [10] Thomas, C., Jennings, P., Lloyd, B. (2008). Issues in renewable energy education. *Australian Journal of Environmental Education*, 24: 67-73. <https://doi.org/10.1017/S0814062600000598>
 - [11] Harsito, C., Purba, D.A., Mufti, R.A.P., Triyono, T., Permata, A.N.S. (2022). Mini review of thermoelectric application with LFP 18650 battery in forest exploration campfire. *AIP Conference Proceedings*, 2499(1): 030001. <https://doi.org/10.1063/5.0104938>
 - [12] Olabi, A.G., Al-Murisi, M., Maghrabie, H.M., Yousef, B.A., Sayed, E.T., Alami, A.H., Abdelkareem, M.A. (2022). Potential applications of thermoelectric generators (TEGs) in various waste heat recovery systems. *International Journal of Thermofluids*, 16: 100249. <https://doi.org/10.1016/j.ijft.2022.100249>
 - [13] Ragupathi, P., Barik, D., Aravind, S., Vignesh, G. (2021). Performance optimization of thermoelectric generators using Taguchi method. *IOP Conference Series: Materials Science and Engineering*, 1059(1): 012053. <https://doi.org/10.1088/1757-899X/1059/1/012053>
 - [14] Jouhara, H., Żabnieńska-Góra, A., Khordehghah, N., Doraghi, Q., et al. (2021). Thermoelectric generator (TEG) technologies and applications. *International Journal of Thermofluids*, 9: 100063. <https://doi.org/10.1016/j.ijft.2021.100063>
 - [15] Shin, S., Bang, S., Choi, J., Son, H.J., et al. (2015). Power generation characteristics of a sandwich-type self-heating thermoelectric generator with spatially varying embedded heat source. *International Journal of Energy Research*, 39(6): 851-859. <https://doi.org/10.1002/er.3285>
 - [16] Saviers, K.R., Hodson, S.L., Fisher, T.S., Salvador, J.R., Kasten, L.S. (2013). Carbon nanotube arrays for enhanced thermal interfaces to thermoelectric modules. *Journal of Thermophysics and Heat Transfer*, 27(3): 474-481. <https://doi.org/10.2514/1.T4026>
 - [17] Kim, M., Yang, H., Wee, D. (2014). Analysis of a sandwich-type generator with self-heating thermoelectric elements. *Energy Conversion and Management*, 81: 440-446. <https://doi.org/10.1016/j.enconman.2014.02.061>
 - [18] Zhang, Y., Feng, B., Hayashi, H., Chang, C.P., et al. (2018). Double thermoelectric power factor of a 2D electron system. *Nature Communications*, 9(1): 2224. <https://doi.org/10.1038/s41467-018-04660-4>
 - [19] Kumar, S.S., Valanarasu, S., Manthrammal, M.A., Shkir, M. (2024). Effect of coating temperature on the physical properties of Bi₂S₃ thin films for photodetector applications. *Journal of Materials Science: Materials in Electronics*, 35(3): 195. <https://doi.org/10.1007/s10854-023-11820-w>
 - [20] Harsito, C., Muslim, R., Rovianto, E., Prasetyo, A. (2023). Investigation of a thermoelectric generator with sandwich leg modification. In *International Conference and Exhibition on Sustainable Energy and Advanced Materials*, Putrajaya, Malaysia, pp. 331-335. https://doi.org/10.1007/978-981-97-0106-3_53
 - [21] Li, M., Zhang, Y., Zhang, T., Zuo, Y., et al. (2021). Enhanced thermoelectric performance of n-type Bi₂Se₃ nanosheets through Sn doping. *Nanomaterials*, 11(7): 1827. <https://doi.org/10.3390/nano11071827>
 - [22] Pei, J., Cai, B., Zhuang, H.L., Li, J.F. (2020). Bi₂Te₃-based applied thermoelectric materials: Research advances and new challenges. *National Science Review*, 7(12): 1856-1858. <https://doi.org/10.1093/nsr/nwaa259>
 - [23] Ngabonziza, P. (2022). Quantum transport and potential of topological states for thermoelectricity in Bi₂Te₃ thin films. *Nanotechnology*, 33(19): 192001. <https://doi.org/10.1088/1361-6528/ac4f17>
 - [24] Ouyang, Z., Li, D. (2016). Modelling of segmented high-performance thermoelectric generators with effects of thermal radiation, electrical and thermal contact resistances. *Scientific Reports*, 6(1): 24123. <https://doi.org/10.1038/srep24123>
 - [25] Guo, C., Zhou, S., Bu, Y., Wang, X. (2023). Modeling and property study of thermoelectric converter based on subwavelength photothermal absorption structure. *Physica B: Condensed Matter*, 664: 415024. <https://doi.org/10.1016/j.physb.2023.415024>
 - [26] Harsito, C., Putra, M.R.A., Purba, D.A., Triyono, T. (2023). Mini review of thermoelectric and their potential applications as coolant in electric vehicles to improve system efficiency. *Evergreen*, 10(1): 469-479. <https://doi.org/10.5109/6782150>
 - [27] Saputro, H., Juwantonono, H., Bugis, H., Wijayanto, D.S., et al. (2018). Numerical simulation of flame stabilization in meso-scale vortex combustion. *MATEC Web of Conferences*, 197: 08005. <https://doi.org/10.1051/mateconf/201819708005>
 - [28] Anggara, B., Widiastuti, I., Saputro, H. (2018). Numerical study of Savonius wind turbine with additional fin blade using computational fluid dynamic. *IOP Conference Series: Materials Science and Engineering*, 434(1): 012172. <https://doi.org/10.1088/1757-899X/434/1/012172>
 - [29] Muslim, R., Saputro, H., Firdani, T., Lasmini, S., et al. (2018). Gasification modelling method using energy Gibbs minimum of palm starch solid waste. *IOP Conference Series: Materials Science and Engineering*, 434(1): 012185. <https://doi.org/10.1088/1757-899X/434/1/012185>
 - [30] Harsito, C., Permana, A.N.S., Sihta, F. (2021). Energy efficiency calculation and air handling unit design based on cooling load capacity at MASTEK Mosque. *IOP Conference Series: Earth and Environmental Science*, 746(1): 012032. <https://doi.org/10.1088/1755-1315/746/1/012032>
 - [31] Harsito, C., Muslim, R., Rovianto, E., Kurniawan, Y., Mahdhudhu, F.M. (2024). Forecasting thermoelectric power generation through utilization of waste heat from building cooling systems based on simulation. *E-Prime-Advances in Electrical Engineering, Electronics and Energy*, 10: 100821. <https://doi.org/10.1016/j.prime.2024.100821>
 - [32] Pramudi, G., Harsito, C., Muslim, R., Adika, D. (2024). Investigation of a thermoelectric generator with sandwich leg modification. *International Journal on Engineering Applications*, 12(2): 87-93. <https://doi.org/10.15866/irea.v12i2.23648>
 - [33] Erturun, U., Mossi, K. (2012). A feasibility investigation on improving structural integrity of thermoelectric modules with varying geometry. *Smart Materials, Adaptive Structures and Intelligent Systems*, 45103: 939-945. <https://doi.org/10.1115/SMASIS2012-8247>
 - [34] Harsito, C., Triyono, T., Rovianto, E. (2022). Analysis of heat potential in solar panels for thermoelectric

generators using ANSYS software. Civil Engineering Journal, 8(7): 1328-1338. <https://doi.org/10.28991/CEJ-2022-08-07-02>

- [35] Aridi, R., Faraj, J., Ali, S., Lemenand, T., Khaled, M. (2021). Thermoelectric power generators: State-of-the-art, heat recovery method, and challenges. Electricity, 2(3): 359-386. <https://doi.org/10.3390/electricity2030022>
- [36] Saidur, R., Rezaei, M., Muzammil, W. K., Hassan, M. H., Paria, S., Hasanuzzaman, M. (2012). Technologies to recover exhaust heat from internal combustion engines. Renewable and sustainable energy reviews, 16(8): 5649-5659. <https://doi.org/10.1016/j.rser.2012.05.018>

NOMENCLATURE

S	seebeck coefficient
V	voltage
T	temperature
K	thermal conductivity, $\text{W.m}^{-1}.\text{K}^{-1}$
I	electrical current (a)
k	boltzmann's constant
P	power generated (w)
A	cross-sectional areas (mm)
R	electrical resistance (ω)
L	thickness
W	electrical power output generated by the TEG

Greek symbols

α	thermal diffusivity, $\text{m}^2.\text{s}^{-1}$
β	thermal expansion coefficient, K^{-1}
ϕ	solid volume fraction
Θ	dimensionless temperature
μ	dynamic viscosity, $\text{kg}.\text{m}^{-1}.\text{s}^{-1}$
Δ	differences
η	efficiency
ρ	resistivity is a material property
σ	electrical conductivity (s/m)

Subscripts

C	cold
E	electron
Max	maximum
H	hot
P	P-type
N	N-type

Abbreviations

TEG	thermoelectric generator
TE	thermo electric
TEM	thermoelectric module
CFD	computational fluid dynamics
FEM	finite element method